Statistics of charge and phase in a ballistic chaotic cavity

A. L. R. Barbosa,[1] A. F. Macedo-Junior,[2] and A. M. S. Macêdo[1]
[1]*Departamento de Física Laboratório de Física Teórica e Computacional, Universidade Federal de Pernambuco, 50670-901 Recife, Pernambuco, Brazil*
[2]*Departamento de Física, Universidade Federal Rural de Pernambuco, 52171-900 Recife, Pernambuco, Brazil*
(Received 25 February 2008; revised manuscript received 6 May 2008; published 10 July 2008)

We study low-frequency current and voltage fluctuations on a two terminal ballistic chaotic cavity coupled to an electromagnetic environment and to two leads with an equal number of propagating modes via barriers of arbitrary transparencies, in the semiclassical regime. We obtain analytical expressions for the charge and phase cumulants for a voltage- and a current-biased cavity, respectively. We observe in the transmitted charge distribution a clear signature of the quantum phase transition reported by Macêdo and Souza [Phys. Rev. E **71**, 066218 (2005)].

DOI: 10.1103/PhysRevB.78.045306 PACS number(s): 73.23.−b, 73.21.La, 05.45.Mt

I. INTRODUCTION

One of the most successful theoretical approaches in mesoscopic physics is the Landauer-Büttiker scattering formalism.[1,2] In the absence of Coulomb interaction, this formalism allows for a complete description of electron dynamics in voltage-biased coherent conductors which encompasses not only the electrical conductance but also the shot-noise power and eventually all high-order cumulants of charge-counting statistics by means of the Levitov-Lesovik determinantal formula.[3]

In the Landauer-Büttiker formalism, a mesoscopic conductor is described by its scattering matrix, or most conveniently, by a set of transmission eigenvalues τ_n, i.e., eigenvalues of the Hermitian matrix $t^\dagger t$, where t is the transmission matrix.[4] In the presence of impurity scattering or chaotic dynamics, the transmission eigenvalues become random variables, and ensemble averages are necessary to make comparisons with experimental data. Since the cumulants of charge are linear statistics of the transmission eigenvalues, their density, defined as $\rho(\tau)=\Sigma_j\langle\delta(\tau-\tau_j)\rangle$, contains all relevant statistical information to obtain these averages. In the semiclassical regime, defined by a large number of scattering channels, the neglect of interference effects implies transport observables with a narrow Gaussian distribution. In this regime, the transmission eigenvalue density and, thus, the transport observables can be conveniently described by means of a quantum circuit theory discovered and developed by Nazarov.[5,6] In this approach, the system is partitioned into three elements: terminals, nodes, and connectors. Appropriate Kirchhoff's laws allow for the determination of the transmission eigenvalue density of the system. In the particular case of two terminal systems, there are two general approaches to construct such a circuit theory: a supermatrix version[7–10] based on the saddle-point structure of the supersymmetric nonlinear sigma model, and a Keldysh version,[11] which is based on the quasiclassical Green's-function approach. It can be shown[6,10] that by employing an appropriate parametrization these approaches are fully equivalent.

In a realistic experimental setup, however, a mesoscopic conductor must be embedded in a macroscopic electrical circuit, which in turn influences the measured transport properties. The classical back-action effects of a linear electromagnetic environment was described in Ref. 12 by means of a field theory constructed from a real-time Keldysh action containing fluctuating potentials. As pointed out in Ref. 12, in the low-frequency limit this field theory becomes local and the functional integral can be evaluated in the saddle-point approximation, thus allowing the calculation of classical back-action effects on the cumulants of charge-counting statistics. The results interpolate between the regimes of voltage bias and current bias and it appears that no equivalent exists for the Levitov-Lesovik formula that could be used to give a statistical interpretation of the crossover region in terms of transmission events. Explicit calculations for a single one-channel barrier were put forward in Ref. 13.

Motivated by these results, we consider in this paper the above described voltage-current bias crossover in a ballistic chaotic cavity, coupled via barriers of arbitrary transparencies to two leads with an equal number of propagation channels. In the standard random-matrix approach, the scattering matrix describing electron transport though such a cavity is distributed according to the Poisson kernel[14] and the semiclassical limit can be accessed by a diagrammatic analysis for performing averages on the unitary group,[15] or equivalently, by a circuit theory approach.[8] Following Ref. 13, the effects of the environment is taken into account by adding an impedance Z in series with the cavity. In particular, we obtain analytical expressions for the distributions of transmitted charge and accumulated phase, for a voltage bias and a current bias cavity, respectively. The voltage-biased cavity was studied in a previous work,[9] which reported the existence of a quantum transition associated with the formation of Fabry-Pérot modes inside the cavity. In this paper, we use the full charge-transfer distribution to characterize this transition. We believe that our results could be of direct experimental interest. The charge-counting statistics of a tunnel junction[16] and of a chaotic quantum dot[17] were recently observed experimentally. In Ref. 17 a method was proposed to count single-electron transfers through a quantum dot by using a quantum point contact as a charge detector. This method allows for a real-time detection which can directly measure the distribution function of transferred electrons as a function of the barriers transparencies, thus making direct contact with the quantity calculated in our work.

The paper is organized as follows: In Sec. II we briefly review the characteristics of voltage- and current-biased mesoscopic conductors, introduce the generating function of cumulants, and show its connection with quantum circuit theory. In Sec. III we formulate the problem in the language of circuit theory and we derive analytical results for cumulants of charge and phase in some particular cases of interest. We also present analytical expressions for the charge and phase distributions, in those particular cases, by using the saddle-point approximation. This approximation is also used to obtain numerically the charge distribution for the general case of arbitrary barriers. Finally, in Sec. IV, we include the effect of the electromagnetic environment by adding an impedance in series with the cavity.

II. CURRENT-VOLTAGE DUALITY

In quantum mechanics, the current I and the voltage V across a given system are described by noncommuting operators. In an observation time T_0, the transmitted charge $q_0=\int_0^{T_0} I(t)dt$ and the accumulated phase $\varphi_0=(e/\hbar)\int_0^{T_0} V(t)dt$ are conjugated operators satisfying the commutation relation $[\varphi_0, q_0]=i\,e$. Such relation is at the origin of the difficulties to treat current-biased conductors in the Landauer-Büttiker formalism.

A. Voltage-biased conductor

In a voltage-biased conductor, electrons are injected into the system with a fixed frequency eV/h and are transmitted at a variable rate $I(t)/e$. The number n of transmitted electrons in a time interval T_0, $n=\int_0^{T_0} dt I(t)/e$, is a random variable with probability distribution P_n, whose cumulant generating function is given by the celebrated Levitov-Lesovik formula of full-counting statistics (FCS),[3]

$$\Phi(\lambda;\{\tau\}) = -M_0 \sum_{j=1}^{N} \ln[1+\tau_j(e^{i\lambda}-1)], \tag{1}$$

where $M_0=eVT_0/h$ is the number of attempts per channel to transmit an electron during the observation time T_0, V is the voltage bias, and N is the number of open scattering channels. Equation (1) contains all information about the charge-counting statistics; in particular, the charge-transfer probability is obtained via the relation

$$P_n(\{\tau\}) = \int_{-\pi}^{\pi} \frac{d\lambda}{2\pi}\, e^{-\Phi(\lambda;\{\tau\})-in\lambda}. \tag{2}$$

Note that Eqs. (1) and (2) depend parametrically on the set $\{\tau_i; i=1,\ldots,N\}$ of transmission eigenvalues that provides the pin-code of the mesoscopic conductor. In the presence of chaotic dynamics or impurity scattering, the transmission eigenvalues become themselves sample dependent random variables, whose joint distribution, in the case of an ergodic ballistic cavity, can be obtained from random-matrix theory.[4] We define the ensemble average

$$\Phi(\lambda) \equiv \langle \Phi(\lambda;\{\tau\})\rangle = -M_0 S(\lambda), \tag{3}$$

where

$$S(\lambda) = \int_0^1 d\tau \rho(\tau) \ln[1+\tau(e^{i\lambda}-1)], \tag{4}$$

in which $\rho(\tau)$ is the average transmission eigenvalue density. The ensemble averaged cumulants of charge counting are given by

$$\langle\langle n^k\rangle\rangle = -\frac{d^k}{d(i\lambda)^k}\Phi(\lambda)\bigg|_{\lambda=0} = M_0 \frac{d^k S(\lambda)}{d(i\lambda)^k}\bigg|_{\lambda=0}. \tag{5}$$

In the same way, the ensemble averaged charge-counting distribution[18] is defined by

$$P_n = \langle P_n(\{\tau\})\rangle = \int_{-\pi}^{\pi} \frac{d\lambda}{2\pi} \langle e^{-\Phi(\lambda;\{\tau\})}\rangle e^{-in\lambda}. \tag{6}$$

Its exact expression depends on the joint distribution of transmission eigenvalues. However, in the semiclassical limit, $N \gg 1$, we can neglect correlations between transmission eigenvalues and use the mean-field approximation

$$\langle e^{-\Phi(\lambda;\{\tau\})}\rangle \approx e^{-\langle\Phi(\lambda;\{\tau\})\rangle} = e^{M_0 S(\lambda)}, \tag{7}$$

to write the ensemble averaged charge-counting distribution as

$$P_n = \int_{-\pi}^{\pi} \frac{d\lambda}{2\pi} e^{M_0 S(\lambda) - in\lambda}. \tag{8}$$

It is convenient to introduce the normalized variable $x=n/\mathcal{M}$ $(0\le x\le 1)$ where $\mathcal{M}=M_0 N$ is the total number of transmission attempts in the observation time. The new distribution is given by

$$\mathcal{P}(x) = \mathcal{M} \int_{-\pi}^{\pi} \frac{d\lambda}{2\pi} e^{\mathcal{M}[\Omega(\lambda)-ix\lambda]}, \tag{9}$$

where we defined $\Omega(\lambda)=S(\lambda)/N$.

B. Current-biased conductor

In the problem of a current-biased conductor, the electrons are transmitted at a fixed rate I/e and have a fluctuating hitting frequency $eV(t)/h$. The number of transmitted charges in the observation time T_0 is, thus, given by $N_0=IT_0/e$. The number of trials m necessary to achieve the transmission rate during the time interval I_0 is $m=\int_0^{T_0} dt\ eV(t)/h=\varphi_0/(2\pi)$, which is a random variable.

It was shown in Ref. 13 that the ensemble averaged cumulants of the accumulated phase have a generating function given formally by

$$\mathcal{G}(\lambda) = iN_0 S^{-1}(-i\lambda), \tag{10}$$

where S^{-1} is the inverse function of S. The ensemble averaged phase cumulants are obtained from

$$\langle\langle m^k\rangle\rangle = -\frac{d^k \mathcal{G}(\lambda)}{d(i\lambda)^k}\bigg|_{\lambda=0}. \tag{11}$$

The full distribution of the number of transmission attempts in the semiclassical limit is obtained from the Fourier transform

$$P_m = \int_{-\pi}^{\pi} \frac{d\lambda}{2\pi} e^{-iN_0 S^{-1}(-i\lambda) - im\lambda}. \tag{12}$$

As in Sec. II A, we define the normalized variable $y = n/\mathcal{N}$ $(1 \leq y < \infty)$, where $\mathcal{N} = N_0/N$ is the total number of transmitted electrons per channel that is fixed by the current bias. After the transformation $\lambda \to N\lambda$, the distribution reads

$$\mathcal{P}(y) = N_0 \int_{-\pi/N}^{\pi/N} \frac{d\lambda}{2\pi} e^{-iN_0[\Omega^{-1}(-i\lambda) + y\lambda]}, \tag{13}$$

where $\Omega^{-1}(\lambda) = S^{-1}(N\lambda)$ is the inverse of $\Omega(\lambda)$.

As we have seen, the cumulant generating functions and the full distributions in the semiclassical limit are completely determined by the function $S(\lambda)$, which depends on the characteristics of the mesoscopic device under consideration. As we will show in Sec. III C, in this regime, $S(\lambda)$ can be conveniently obtained using circuit theory.

C. Counting statistics and circuit theory

The semiclassical limit of a great number of open channels, $N \gg 1$, is characterized by neglecting quantum interference effects on transport observables. In such regime, the scalar version of circuit theory[5,7] is a very convenient analytical tool to access information contained in the average transmission density; thus, transport properties such as the average conductance, the average shot-noise power, or higher cumulants of the charge-counting statistics can be calculated.

Recently the scalar version of circuit theory was derived both from the saddle-point of a supersymmetric nonlinear σ model[10] and from the Keldysh approach.[6] Following the usual assumptions of circuit theory, the system, composed of connectors and nodes, is supposed to be subject to a pseudopotential ϕ and is traversed by a pseudocurrent given by

$$I(\phi) = \sin(\phi) F(\phi), \quad F(\phi) = \int_0^1 d\tau \frac{\rho(\tau)\tau}{1 - \tau \sin^2(\phi/2)}. \tag{14}$$

The "current-voltage" characteristics of the connectors are taken as input, and a pseudocurrrent conservation law in the nodes allows for the calculation of the pseudocurrent, given by Eq. (14), of the whole system.

The pseudocurrent can be used to obtain the cumulants of the charge-counting statistics, since it can be related to action (4). In order to establish such a connection, we define the auxiliary function

$$g(\varepsilon) \equiv -i \left. \frac{\partial S(\lambda)}{\partial \lambda} \right|_{e^{i\lambda} = 1 - \varepsilon^2} = \int_0^1 d\tau \frac{(1 - \varepsilon^2)\rho(\tau)\tau}{1 - \varepsilon^2 \tau}. \tag{15}$$

From Eqs. (4) and (15), we see that the auxiliary function $g(\varepsilon)$ can be constructed directly from the pseudocurrent as

$$g(\varepsilon) = (1 - \varepsilon^2) F(\phi)|_{\sin(\phi/2) = \varepsilon}, \tag{16}$$

thus

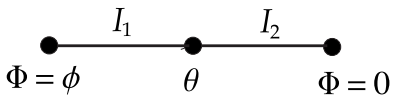

FIG. 1. Circuit representation.

$$g(\varepsilon) = \left. \frac{\sqrt{1 - \varepsilon^2}}{2\varepsilon} I(\phi) \right|_{\sin(\phi/2) = \varepsilon}. \tag{17}$$

The charge cumulants can be obtained from $g(\varepsilon)$ through the formula

$$\langle\langle n^{l+1} \rangle\rangle = M_0 \left(\frac{\varepsilon^2 - 1}{2\varepsilon} \frac{d}{d\varepsilon} \right)^l g(\varepsilon) \Big|_{\varepsilon = 0}. \tag{18}$$

On the other hand, we can also obtain the action via the integral

$$S(\lambda) = i \int_0^{\lambda} d\lambda' g(\varepsilon)|_{\varepsilon^2 = 1 - e^{i\lambda'}}. \tag{19}$$

In this way we established a direct connection between FCS and quantum circuit theory. In Sec. III we shall apply this procedure to study the FCS of a chaotic cavity with two barriers of arbitrary transparencies.

III. CHAOTIC CAVITY WITH BARRIERS OF ARBITRARY TRANSPARENCY

Now we restrict our analysis to a chaotic cavity sandwiched between two barriers. In the circuit theory approach, this system is represented by tree nodes and two connectors, as shown in Fig. 1.

The central node represents the cavity and the connectors correspond to the barriers. The current-voltage characteristics for a general connector consisting of a barrier of arbitrary transparency were obtained in Ref. 7. For the particular case of N equivalent channels on each lead, it can be written as

$$I_j(\phi) = \frac{2N\Gamma_j \tan(\phi/2)}{1 + (1 - \Gamma_j)\tan^2(\phi/2)}, \tag{20}$$

where Γ_j $(j = 1, 2)$ is a phenomenological parameter characterizing the barrier transparency. The pseudocurrent conservation law at the central node reads

$$I(\phi) = I_1(\phi - \theta) = I_2(\theta), \tag{21}$$

Substituting Eq. (20) into Eq. (21) yields

$$\frac{2N\Gamma_1 \tan(\phi/2 - \theta/2)}{1 + (1 - \Gamma_1)\tan^2(\phi/2 - \theta/2)} = \frac{2N\Gamma_2 \tan(\theta/2)}{1 + (1 - \Gamma_2)\tan^2(\theta/2)}. \tag{22}$$

By introducing the variables $\xi = \tan\theta/2$ and $\eta = \tan\phi/2$, we can write Eq. (22) as a fourth-order polynomial equation,

$$\Gamma_1(1-\Gamma_2)\eta\xi^4+[\Gamma_1+\Gamma_2-\eta^2(\Gamma_1-\Gamma_2+\Gamma_1\Gamma_2)]\xi+[\Gamma_1+\Gamma_2-2\Gamma_1\Gamma_2+\eta^2(\Gamma_1\Gamma_2+\Gamma_2-\Gamma_1)]\xi^3+3\eta\Gamma_1\Gamma_2\xi^2-\eta\Gamma_1=0, \tag{23}$$

the physical solution of which, denoted by ξ_{sol}, determines the pseudocurrent of the system,

$$I(\phi)=\frac{2N\Gamma_2\xi_{\mathrm{sol}}}{1+(1-\Gamma_2)\xi_{\mathrm{sol}}^2}, \tag{24}$$

which, in turn, is used to construct the action $S(\lambda)$ by using formulas (17) and (19).

The general analytical solution of Eq. (23) is so cumbersome that it loses its utility in finding an exact expression for $S(\lambda)$. We postpone solving this problem by treating particular cases for which the action can be written in closed form.

A. Symmetric barriers

In this particular case we set $\Gamma_1=\Gamma_2=\Gamma$, and Eq. (23) simplifies to

$$(\eta\xi^2+2\xi-\eta)[(1-\Gamma)\xi^2+\Gamma\eta\xi+1]=0. \tag{25}$$

The physical solution is given by

$$\xi_{\mathrm{sol}}=\frac{1}{\eta}(-1+\sqrt{1+\eta^2}). \tag{26}$$

Therefore, we can write the auxiliary function as

$$g(\varepsilon)=\frac{N\Gamma(1-\varepsilon^2)}{(2-\Gamma)\sqrt{1-\varepsilon^2}+\Gamma(1-\varepsilon^2)}, \tag{27}$$

and, using Eq. (19), we obtain the action

$$S(\lambda)=2N\ln\left[1+\frac{\Gamma}{2}(e^{i\lambda/2}-1)\right]. \tag{28}$$

These expressions can be used to obtain all cumulants of the charge-counting statistics. For instance, the first four cumulants are given by

$$\langle\langle n\rangle\rangle=M_0N\frac{\Gamma}{2}, \tag{29}$$

$$\langle\langle n^2\rangle\rangle=M_0N\frac{\Gamma(2-\Gamma)}{8}, \tag{30}$$

$$\langle\langle n^3\rangle\rangle=M_0N\frac{\Gamma(1-\Gamma)(2-\Gamma)}{16}, \tag{31}$$

$$\langle\langle n^4\rangle\rangle=M_0N\frac{\Gamma(2-\Gamma)(3\Gamma^2-6\Gamma+2)}{64}. \tag{32}$$

Apart from the cumulants, Eq. (28) can be used to obtain the full distribution of transmitted charge. Since $\mathcal{M}\gg 1$ we can treat the variable x in Eq. (9) as a continuous variable and evaluate the integral by a saddle-point approximation. Expanding around the saddle point up to second order, we obtain the following normalized distribution:

$$\mathcal{P}(x)=\sqrt{\frac{\mathcal{M}}{\pi x(1-x)}}\left[\frac{\Gamma^x(2-\Gamma)^{1-x}}{2x^x(1-x)^{1-x}}\right]^{2\mathcal{M}}. \tag{33}$$

The same steps can be taken to obtain the voltage distribution. In this case, we need the inverse action, which is easily obtained from Eq. (28), yielding

$$\mathcal{S}^{-1}(\lambda)=-2i\ln\left[1+\frac{2}{\Gamma}(e^{\lambda/2N}-1)\right]. \tag{34}$$

The cumulants are obtained from the generating function $\mathcal{G}(\lambda)=iN_0\mathcal{S}^{-1}(-i\lambda)$. The first four cumulants are

$$\langle\langle m\rangle\rangle=\frac{2N_0}{N\Gamma}, \tag{35}$$

$$\langle\langle m^2\rangle\rangle=\frac{N_0(2-\Gamma)}{N^2\Gamma^2}, \tag{36}$$

$$\langle\langle m^3\rangle\rangle=\frac{N_0(2-\Gamma)(4-\Gamma)}{2N^3\Gamma^3}, \tag{37}$$

$$\langle\langle m^4\rangle\rangle=\frac{N_0(2-\Gamma)(24-12\Gamma+\Gamma^2)}{4N^4\Gamma^4}. \tag{38}$$

The full voltage distribution is obtained by evaluating integral (13) in the saddle-point approximation, which yields

$$\mathcal{P}(y)=\sqrt{\frac{N_0}{\pi y(y-1)}}\left[\frac{\Gamma y^y(2-\Gamma)^{y-1}}{2^y(y-1)^{y-1}}\right]^{2N_0}. \tag{39}$$

B. Tunnel junctions

Applying the condition $\Gamma_1,\Gamma_2\ll 1$ to Eq. (23), it simplifies to

$$(\xi^2+1)(\xi^2+a\xi-1)=0, \tag{40}$$

where $a=[\Gamma_1+\Gamma_2-\eta^2(\Gamma_1-\Gamma_2)]/\Gamma_1\eta$. With the physical solution we can write

$$g(\varepsilon)=\frac{N\Gamma_1\Gamma_2(1-\varepsilon^2)}{\sqrt{(\Gamma_1+\Gamma_2)^2-4\Gamma_1\Gamma_2\varepsilon^2}}, \tag{41}$$

and thus the action reads

$$S(\lambda)=\frac{N}{2}[\sqrt{(\Gamma_1+\Gamma_2)^2+4\Gamma_1\Gamma_2(e^{i\lambda}-1)}-\Gamma_1-\Gamma_2], \tag{42}$$

in agreement with Ref. 19 and confirmed by the experiments in Ref. 17. These equations allow us to obtain the cumulants of the charge-counting statistics. The first ones are given below:

$$\langle\langle n\rangle\rangle=M_0N\frac{\Gamma_1\Gamma_2}{\Gamma_1+\Gamma_2}, \tag{43}$$

$$\langle\langle n^2\rangle\rangle=M_0N\frac{\Gamma_1\Gamma_2(\Gamma_1^2+\Gamma_2^2)}{(\Gamma_1+\Gamma_2)^3}, \tag{44}$$

$$\langle\langle n^3\rangle\rangle = M_0 N\Gamma_1\Gamma_2(\Gamma_1+\Gamma_2)^{-5} \times(\Gamma_1^4 - 2\Gamma_1^3\Gamma_2 + 6\Gamma_1^2\Gamma_2^2 - 2\Gamma_1\Gamma_2^3 + \Gamma_2^4), \quad (45)$$

$$\langle\langle n^4\rangle\rangle = M_0 N\Gamma_1\Gamma_2(\Gamma_1+\Gamma_2)^{-7}(\Gamma_1^6 - 8\Gamma_1^5\Gamma_2 + 31\Gamma_1^4\Gamma_2^2 - 40\Gamma_1^3\Gamma_2^3 + 31\Gamma_1^2\Gamma_2^4 - 8\Gamma_1\Gamma_2^5 + \Gamma_2^6). \quad (46)$$

In Ref. 17 the authors obtained experimentally the charge distribution, which shows excellent agreement with a numerical integration of Eq. (8) with $S(\lambda)$ given by Eq. (42). Such distribution can also be obtained via the saddle-point approximation. The distribution of the normalized charge $x=n/\mathcal{M}$ in the particular case $\Gamma_1=\Gamma_2=\Gamma$ is given by

$$P(x) = \sqrt{\frac{\mathcal{M}}{\pi x}}\exp\{\mathcal{M}[2x - \Gamma - 2x\ln(2x/\Gamma)]\}. \quad (47)$$

The general case $\Gamma_1 \neq \Gamma_2$ is shown in Appendix B.

To study the statistics of accumulated phase, it is necessary to obtain the inverse of $S(\lambda)$. In our case the inverse of Eq. (42) is

$$S^{-1}(\lambda) = -i\ln\left[1 + \frac{\lambda^2 + \lambda N(\Gamma_1+\Gamma_2)}{\Gamma_1\Gamma_2 N^2}\right]. \quad (48)$$

The cumulants are easily obtained by differentiating the generating function $\mathcal{G}(\lambda)=iN_0S^{-1}(-i\lambda)$. The first four cumulants are listed below:

$$\langle\langle m\rangle\rangle = \frac{N_0(\Gamma_1+\Gamma_2)}{N\Gamma_1\Gamma_2}, \quad (49)$$

$$\langle\langle m^2\rangle\rangle = \frac{N_0(\Gamma_1^2+\Gamma_2^2)}{N^2\Gamma_1^2\Gamma_2^2}, \quad (50)$$

$$\langle\langle m^3\rangle\rangle = \frac{2N_0(\Gamma_1+\Gamma_2)(\Gamma_1^2+\Gamma_2^2-\Gamma_1\Gamma_2)}{N^3\Gamma_1^3\Gamma_2^3}, \quad (51)$$

$$\langle\langle m^4\rangle\rangle = \frac{6N_0(\Gamma_1^4+\Gamma_2^4)}{N^4\Gamma_1^4\Gamma_2^4}. \quad (52)$$

The full distribution of accumulated phase is given by integral (13), which can be evaluated in the saddle-point approximation. In the particular case $\Gamma_1=\Gamma_2=\Gamma$, the distribution is given by

$$\mathcal{P}(y) = \sqrt{\frac{N_0}{\pi y^2}}\exp\{N_0[2 - \Gamma y + 2\ln(\Gamma y/2)]\}. \quad (53)$$

The general expression for $\Gamma_1 \neq \Gamma_2$ is given in Appendix B.

C. Barriers of arbitrary transparency

In the general case of barriers with arbitrary transparencies, we have to solve quartic equation (23). The analytical solution is too cumbersome and not useful for explicit cumulant calculations. Nevertheless, we can construct the physical root as a power series in ε, which is achieved by inserting the *Ansätze*

$$\xi_{\rm sol} = a_0 + a_1\varepsilon + a_2\varepsilon^2 + \cdots, \quad (54)$$

$$\eta = \tan\phi/2 = \frac{\varepsilon}{\sqrt{1-\varepsilon^2}} = \varepsilon + \frac{1}{2}\varepsilon^3 + \frac{3}{8}\varepsilon^5 + \cdots \quad (55)$$

into Eq. (23). Equating terms with the same powers of ε, we obtain recursive equations for the coefficients, which can be easily solved, yielding $a_1=0$, $a_2=\Gamma_1/(\Gamma_1+\Gamma_2)$, $a_3=0$, and so on. Inserting the above constructed solution into Eq. (24) and using relation (17), we obtain a series expansion for $g(\varepsilon)$. Finally, a series expansion for $S(\lambda)$ is obtained by means of integral (19). With this procedure, we can easily obtain the cumulants by using Eq. (5) and (18). The first two cumulants are listed below:

$$\langle n\rangle = \frac{M_0 N\Gamma_1\Gamma_2}{\Gamma_1+\Gamma_2}, \quad (56)$$

$$\langle\langle n^2\rangle\rangle = \frac{M_0 N\Gamma_1\Gamma_2(\Gamma_1+\Gamma_2-\Gamma_1\Gamma_2)(\Gamma_1^2+\Gamma_2^2)}{(\Gamma_1+\Gamma_2)^4}. \quad (57)$$

The third and fourth cumulants are presented in Appendix A. Note that Eqs. (56) and (57) reduce to Eqs. (29) and (30) in the particular case of symmetric barriers $\Gamma_1=\Gamma=\Gamma_2$, and to Eqs. (43) and (44) in the case of tunnel junctions $\Gamma_1,\Gamma_2 \ll 1$.

Now we turn our attention to the dual problem of a current-biased circuit. Although we do not have a close expression for $S(\lambda)$, we can write its inverse as a series expansion, $S^{-1}(\lambda)=b_0+b_1\lambda+b_2\lambda^2+\cdots$, whose coefficients are directly obtained from the series expansion of $S(\lambda)$. Such expansion is sufficient to obtain the cumulants of the statistics of accumulated phase. The first two cumulants are given below:

$$\langle m\rangle = \frac{N_0(\Gamma_1+\Gamma_2)}{N\Gamma_1\Gamma_2}, \quad (58)$$

$$\langle\langle m^2\rangle\rangle = \frac{N_0(\Gamma_1^2+\Gamma_2^2)(\Gamma_1+\Gamma_2-\Gamma_1\Gamma_2)}{N^2\Gamma_1^2\Gamma_2^2(\Gamma_1+\Gamma_2)}. \quad (59)$$

The next two cumulants are also given in Appendix A. Note that Eqs. (58) and (59) simplify to Eqs. (35) and (36) in the particular case of symmetric barriers and to Eqs. (49) and (50) in the case of tunnel junctions.

In this general case, analytical calculations are limited to calculating cumulants; however, we can still obtain the full distribution $\mathcal{P}(x)$ or, more conveniently, its logarithm, defined as

$$W(x) = \frac{1}{\mathcal{M}}\ln\mathcal{P}(x), \quad (60)$$

by a numerical implementation of the saddle-point approximation. Such numerical results are shown in Sec. III B, in which we study the effects of a recently reported quantum transition on the functional form of $W(x)$.

We remark that in the semiclassical limit and for a great number of transmission attempts, i.e., $\mathcal{M}=NM \gg 1$, the saddle-point approximation of $\mathcal{P}(x)$ contains all relevant information for cumulant calculations. Numerically obtained cumulants from Eqs. (33) and (47) have excellent agreement with the respective analytical expressions. In fact, we

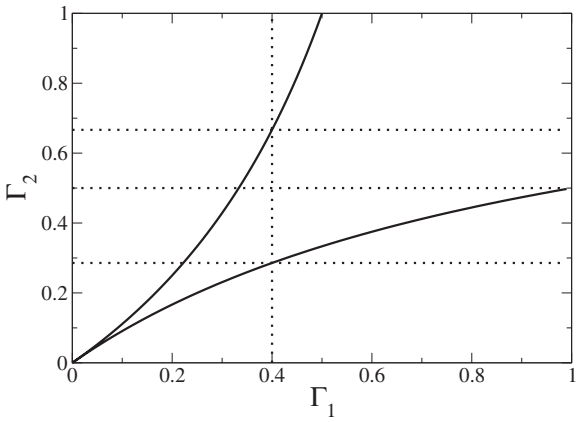

FIG. 2. Diagram illustrating transition lines between transport regimes as functions of the tunnel probabilities. The dotted lines show that for $\Gamma_1=1$ there is a transition point at $\Gamma_2=0.5$. On the other hand, for $\Gamma_1=0.4$ there are transitions at the points $\Gamma_2\approx 0.28$ and $\Gamma_2\approx 0.67$.

checked that the analytical results can be directly obtained from the function $W(x)$. For example, the first-order cumulant is obtained from the minimum condition

$$\left.\frac{dW(x)}{dx}\right|_{x=\bar{x}} = 0 \quad \Rightarrow \quad \bar{x} = n_1, \tag{61}$$

where we introduced the notation $n_k=\langle\langle n^k\rangle\rangle/\mathcal{M}$. The second and third cumulants satisfy the relation

$$n_k = -(-n_2)^k \left.\frac{d^k W(x)}{dx^k}\right|_{x=\bar{x}}, \quad k=2,3. \tag{62}$$

Similar relations are valid for phase cumulants.

D. Signature of a quantum transition

Electron transport in a double-barrier chaotic quantum dot was studied in the semiclassical limit in Ref. 9, by means of the scalar circuit theory. This work reported a quantum transition associated with the formation of Fabry-Pérot modes inside the dot, which is characterized by the emergence of a square-root singularity on the transmission eigenvalue density $\rho(\tau)$ at $\tau=1$. The presence or absence of this singularity characterizes two broad regimes of quantum transport, which can be obtained by varying the barriers' transparencies Γ_1 and Γ_2. The transition lines between these regimes on the $\Gamma_1\Gamma_2$ plane are shown in Fig. 2, and the region between the lines corresponds to the regime characterized by the existence of Fabry-Pérot resonances.

Albeit it contains all relevant information about the transport problem, the transmission eigenvalue density is not directly observable. Therefore, it is important to describe the above quantum transition in terms of experimentally accessible quantities. In Ref. 20 this was achieved by considering the effects of weak Coulomb interactions in the cavity. In Secs. III D 1 and III D 2, we fulfill this requirement for noninteracting cavities by investigating signatures of the quantum transition on the distribution curve for charge transfer. Recent measurements of this quantity[17] provide us with the necessary motivation.

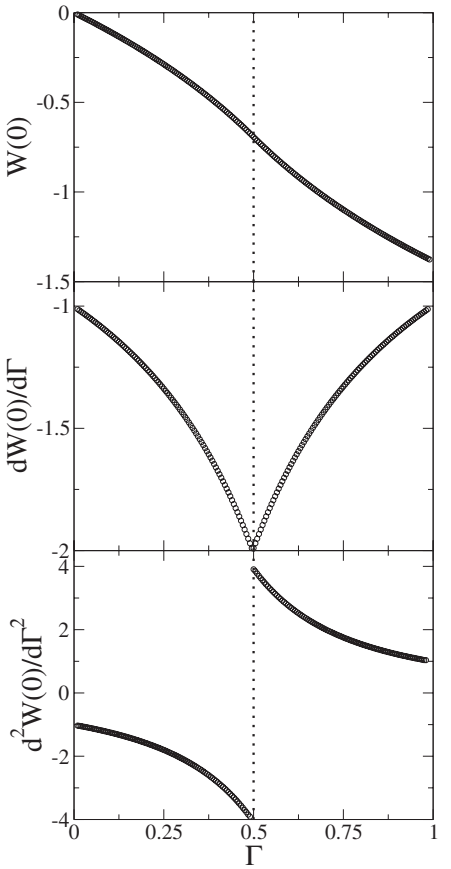

FIG. 3. Signature of the transition. The top graph shows the left border of the charge distribution function as function of Γ. The middle and bottom graphs show the first and second derivatives, respectively. Note that the second derivative is discontinuous precisely at $\Gamma=0.5$ (dotted lines), in agreement with Fig. 2.

1. Quantum dot with an ideal contact and one barrier of arbitrary transparency

This is the simplest case in which the transition occurs. We have one ideal contact, $\Gamma_1=1$, and a barrier of arbitrary transparency, $\Gamma_2=\Gamma$. According to Fig. 2 the transition occurs exactly at $\Gamma_2=0.5$. We study the behavior of the function $W(x)$, at the transition point.

The bulk of the distribution does not present any signal of the transition, as can be verified from the first four cumulants, obtained by setting $\Gamma_1=1$ and $\Gamma_2=\Gamma$ in Eqs. (56), (57), (A3), and (A4), which are smooth functions of Γ. On the other hand, to access information contained on higher cumulants, we need to study the tails of the distribution, i.e., the limits of low transmission, $x\to 0^+$, and high transmission, $x\to 1^-$. In the last limit, we checked that $W(1)$ is a continuous function of Γ, with continuous derivatives, and thus, does not exhibit features of the transition. On the other hand, at the opposite limit, $W(0)$ clearly exhibits the signature we are looking for exactly at $\Gamma=0.5$, as shown in Fig. 3, in which

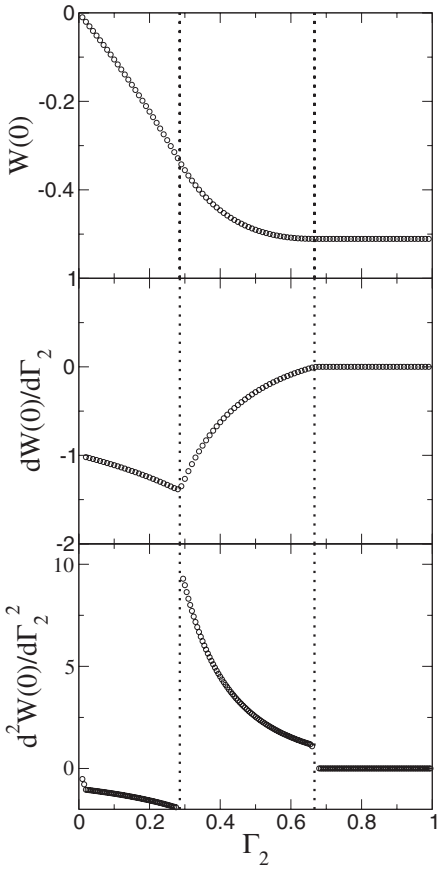

FIG. 4. Left border of the charge distribution (top) and its first (middle) and second (bottom) derivatives. The second derivative shows discontinuities at $\Gamma_2 \approx 0.28$ and $\Gamma_2 \approx 0.67$ according to predictions in Fig. 2.

we plot the left border of the distribution function and its first two derivatives.

The same analysis is valid for the logarithm of the voltage distribution $\bar{W}(y)$, which has support on the interval $1 \leq y < \infty$. Since the bulk of $\bar{W}(y)$ is not relevant, we concentrate on its values on the borders. At the left border, it does not present any signal of the transition. On the other border, it diverges, $\lim_{x\to\infty} \bar{W}(x) = \infty$. This behavior makes the information about transition to be lost.

2. Quantum dot with two barriers of arbitrary transparencies

This is the more general case described by Eq. (23). As discussed above, we search for signals of the transition by studying the tails of $W(x)$. For example, choosing $\Gamma_1 = 0.4$, we plot its right border limit, $W(0)$, and its first two derivatives as a function of Γ_2. As shown in Fig. 4 the second derivative presents discontinuities at $\Gamma_2 \approx 0.28$ and $\Gamma_2 \approx 0.67$, which is in agreement with the analysis on the $\Gamma_1\Gamma_2$ plane shown in Fig. 2. At such values of transparency, the phase transition between different transport regimes is expected to occur.

As discussed in Sec. III D 1, in the high transmission limit $W(1)$ does not show signs of the transition. The same occurs at the left border value $\bar{W}(1)$. In the other limit, $y \to \infty$, $\bar{W}(y)$ diverges and hides the signatures of the transition.

IV. EFFECTS OF THE ELECTROMAGNETIC ENVIRONMENT AND DUALITY RELATIONS

In realistic current and voltage measurements, the mesoscopic conductor is embedded in an external electric circuit, which affects the measured transport observables. A comprehensive theory accounting for the electromagnetic environment was put forward in Ref. 13, which considered a mesoscopic conductor in series with an impedance $Z(\omega)$.

The main result of Ref. 13 concerns the zero-frequency limit, in which the authors present a procedure to present the cumulant generating function of charge cumulants, which in our notation reads

$$\Phi(\lambda) = \frac{M_0}{z_0}[\sigma(\lambda) - i\lambda], \quad \sigma + z_0 S(-i\sigma) = i\lambda, \tag{63}$$

where z_0 is the dimensionless zero-frequency impedance of the external circuit. Note that in the limit $z_0 \to 0$, we have $\Phi(\lambda) = -M_0 S(\lambda)$, which corresponds to the case studied in Sec. III C. The charge cumulants in this limit are now denoted by $\langle\langle n^k \rangle\rangle_0$.

We can construct a power series for $\Phi(\lambda)$ by using the power series of $S(\lambda)$ in Eq. (63). Therefore we are able to calculate the cumulants of the charge-transfer statistics for a chaotic quantum dot in series with a resistor z_0. The first four cumulants are listed below:

$$\langle n \rangle = \frac{\langle n \rangle_0}{1 + g z_0}, \tag{64}$$

$$\langle\langle n^2 \rangle\rangle = \frac{\langle\langle n^2 \rangle\rangle_0}{(1 + g z_0)^3}, \tag{65}$$

$$\langle\langle n^3 \rangle\rangle = \frac{\langle\langle n^3 \rangle\rangle_0}{(1 + g z_0)^4} - \frac{3 g z_0}{1 + g z_0} \frac{\langle\langle n^2 \rangle\rangle_0^2}{\langle n \rangle_0}, \tag{66}$$

$$\langle\langle n^4 \rangle\rangle = \frac{\langle\langle n^4 \rangle\rangle_0}{(1 + g z_0)^5} - \frac{10 g z_0}{(1 + g z_0)^6} \frac{\langle\langle n^2 \rangle\rangle_0 \langle\langle n^3 \rangle\rangle_0}{\langle n \rangle_0} + \frac{15 (g z_0)^2}{(1 + g z_0)^7} \frac{\langle\langle n^2 \rangle\rangle_0^3}{\langle n \rangle_0^2}, \tag{67}$$

where we defined $g = N\Gamma_1\Gamma_2/(\Gamma_1 + \Gamma_2)$ as the dimensionless conductance of the cavity. The same relations were obtained in Ref. 13.

It was also shown in Ref. 13 that the presence of the resistor allows for a simple relation between the cumulants of charge and phase, which in turn implies a simple relation between $\Phi(\lambda)$ and $\mathcal{G}(\lambda)$. It follows that the phase cumulant generating function satisfies

$$\mathcal{G}(\lambda) = g_0 M_0 \zeta(\lambda), \quad g_0 \zeta + S(-i\zeta) = -i\lambda, \tag{68}$$

where we defined $g_0 = 1/z_0$. In the limit $z_0 \to \infty$ ($g_0 \to 0$), it reduces to $\mathcal{G}(\lambda) = -iN_0 S^{-1}(-i\lambda)$, which is the case studied in the previous sections

We can also obtain a power series expansion for $\mathcal{G}(\lambda)$ and in this way obtain the cumulants of the accumulated phase statistics. The first four cumulants are

$$\langle m\rangle = \frac{\langle m\rangle_0}{1+g_0\rho}, \tag{69}$$

$$\langle\langle m^2\rangle\rangle = \frac{\langle\langle m^2\rangle\rangle_0}{(1+g_0\rho)^3}, \tag{70}$$

$$\langle\langle m^3\rangle\rangle = \frac{\langle\langle m^3\rangle\rangle_0}{(1+g_0\rho)^4} - \frac{3g_0\rho}{1+g_0\rho}\frac{\langle\langle m^2\rangle\rangle_0^2}{\langle m\rangle_0}, \tag{71}$$

$$\langle\langle m^4\rangle\rangle = \frac{\langle\langle m^4\rangle\rangle_0}{(1+g_0\rho)^5} - \frac{10g_0\rho}{(1+g_0\rho)^6}\frac{\langle\langle m^2\rangle\rangle_0\langle\langle m^3\rangle\rangle_0}{\langle m\rangle_0} + \frac{15(g_0\rho)^2}{(1+g_0\rho)^7}\frac{\langle\langle m^2\rangle\rangle_0^3}{\langle m\rangle_0^2}, \tag{72}$$

where $\rho=1/g$ is the dimensionless resistance of the cavity and the subscript 0 denotes that it corresponds to the limit $g_0=0$. By comparing Eqs. (64)–(67) and (69)–(72), we note that the dual problems are simply related by making the simple substitution $n\leftrightarrow m$ and $z_0G\leftrightarrow g_0\rho$.

V. CONCLUSIONS

We studied voltage and current fluctuations in a two terminal ballistic chaotic cavity coupled to an electromagnetic environment and to two electron reservoirs via barriers of arbitrary transparency and with a large number of transmission channels. We obtained analytical results for charge and phase cumulants for voltage- and current-biased circuits, which include analytical expressions for the full distributions in the particular cases of symmetric barriers and for tunnel junctions. In addition, we showed how the charge distribution can be used to detect, by varying the barriers transparency, the phase transition reported in Ref. 9 associated with the formation of Fabry-Pérot modes inside the cavity. The transition affects higher-order cumulants and is observed at the tail of the distribution corresponding to the limit of low transmission. We believe that such transition may become experimentally accessible with the development of novel techniques to measure charge-transfer distributions. Recent progress in measurement techniques[16,17] provides ground for some optimism. In order to facilitate eventual comparison with experimental data, we estimated the robustness of the transition by introducing a random fluctuation on the barriers' parameters, thereby allowing the charge distribution $W(x)$ to acquire more realistic precision. We also extended the analysis to a finite interval in the support of $W(x)$ including the extremal point $x=0$. To be specific, in the case presented in Sec. I, we introduced a fluctuation of 5% on the barrier parameter Γ and still observed a clear signature of the transition over a range on the order of 30% of the average value $\bar{x}$. Under these conditions, the estimation of the transition point shows an error of just 14% relative to its exact value $\Gamma_c=0.5$. Under realistic experimental conditions, one should also expect some broadening of the transition due to mesoscopic fluctuations, which were neglected in our semiclassical analysis. The strength of this broadening can be estimated by numerical simulations and are found to be quite small.[9] We also studied classical back-action effects by connecting the cavity in series with an impedance. Relating the obtained charge cumulants to the ones obtained at voltage bias, we recover the same relations obtained in Ref. 13 for a single barrier, which indicate the remarkable universality of the dependency of the measured cumulants on the lower-order ones. We repeated the same reasoning to voltage cumulants and showed that these dual problems are simply related.

ACKNOWLEDGMENTS

This work was partially supported by CNPq and FACEPE (Brazilian agencies).

APPENDIX A: PHASE AND CHARGE CUMULANTS

The third- and fourth-order phase cumulants in the regime $z_0\to\infty$ are given by Eqs. (A1) and (A2). Furthermore, the third- and fourth-order charge cumulants in the regime $z_0\to 0$ are given by Eqs. (A3) and (A4):

$$\langle\langle m^3\rangle\rangle_0 = N_0(\Gamma_1^5\Gamma_2 - 2\Gamma_1^5 + 4\Gamma_1^4\Gamma_2^2 - 4\Gamma_1^4\Gamma_2 - 6\Gamma_1^3\Gamma_2^3 - 2\Gamma_1^3\Gamma_2^2 + 4\Gamma_1^2\Gamma_2^4 - 2\Gamma_1^2\Gamma_2^3 + \Gamma_1\Gamma_2^5 - 4\Gamma_1\Gamma_2^4 - 2\Gamma_2^5) \times(\Gamma_1\Gamma_2 - \Gamma_1 - \Gamma_2)/[N^3\Gamma_1^3\Gamma_2^3(\Gamma_1+\Gamma_2)^3], \tag{A1}$$

$$\langle\langle m^4\rangle\rangle_0 = N_0[(55\Gamma_1^4\Gamma_2^6 + 4\Gamma_1^3\Gamma_2^7 + \Gamma_1^2\Gamma_2^8 - 54\Gamma_1^3\Gamma_2^6 - 30\Gamma_1^2\Gamma_2^7 - 112\Gamma_1^5\Gamma_2^5 + 55\Gamma_1^6\Gamma_2^4 - 54\Gamma_1^6\Gamma_2^3 - 30\Gamma_1^7\Gamma_2^2 - 6\Gamma_1\Gamma_2^8 + \Gamma_1^8\Gamma_2^2 + 4\Gamma_1^7\Gamma_2^3 - 6\Gamma_1^8\Gamma_2^2 + 42\Gamma_1^4\Gamma_2^5 + 42\Gamma_1^5\Gamma_2^4 + 6\Gamma_2^8 + 36\Gamma_1^2\Gamma_2^6 + 24\Gamma_1\Gamma_2^7 + 24\Gamma_1^5\Gamma_2^3 + 36\Gamma_1^6\Gamma_2^2 + 24\Gamma_1^7\Gamma_2 + 12\Gamma_1^4\Gamma_2^4 + 6\Gamma_1^8 + 24\Gamma_1^3\Gamma_2^5)(\Gamma_1+\Gamma_2-\Gamma_1\Gamma 2)]/[N^4\Gamma_1^4\Gamma_2^4(\Gamma_1+\Gamma_2)^5], \tag{A2}$$

$$\langle\langle n^3\rangle\rangle_0 = M_0N\frac{\Gamma_1\Gamma_2(\Gamma_1^4 - 2\Gamma_1^3\Gamma_2 + 6\Gamma_1^2\Gamma_2^2 - 2\Gamma_1\Gamma_2^3 + \Gamma_2^4)(\Gamma_1+\Gamma_2-\Gamma_1\Gamma_2)(\Gamma_1+\Gamma_2-2\Gamma_1\Gamma_2)}{(\Gamma_1+\Gamma_2)^7}, \tag{A3}$$

$$\langle\langle n^4\rangle\rangle_0 = M_0 N[\Gamma_1\Gamma_2(6\Gamma_1^2\Gamma_1^8 - 6\Gamma_1\Gamma_2^8 + \Gamma_2^8 - 36\Gamma_1^3\Gamma_2^7 + 30\Gamma_1^2\Gamma_2^7 - 6\Gamma_1\Gamma_2^7 + 150\Gamma_1^4\Gamma_2^6 - 114\Gamma_1^3\Gamma_2^6 + 16\Gamma_1^2\Gamma_2^6 - 192\Gamma_1^5\Gamma_2^5 + 42\Gamma_1^4\Gamma_2^5 + 14\Gamma_1^3\Gamma_2^5 + 150\Gamma_1^6\Gamma_2^4 + 42\Gamma_1^5\Gamma_2^4 - 18\Gamma_1^4\Gamma_2^4 - 36\Gamma_1^7\Gamma_2^3 - 114\Gamma_1^6\Gamma_2^3 + 14\Gamma_1^5\Gamma_2^3 + 6\Gamma_1^8\Gamma_2^2 + 30\Gamma_1^7\Gamma_2^2 + 16\Gamma_1^6\Gamma_2^2 - 6\Gamma_1^8\Gamma_2 - 6\Gamma_1^7\Gamma_2 + \Gamma_1^8)(\Gamma_1 + \Gamma_2 - \Gamma_1\Gamma_2)]/(\Gamma_1 + \Gamma_2)^{10}. \quad \text{(A4)}$$

APPENDIX B: ASYMMETRIC TUNNEL JUNCTIONS

The charge distribution in the case of asymmetric tunnel junctions can be written as $\mathcal{P}(x) = C(x)e^{\mathcal{M}W(x)}$, where

$$C(x) = \sqrt{\frac{\mathcal{M}[\sqrt{4x^2 + (\Gamma_1 - \Gamma_2)^2} + 2x]}{2\pi x\sqrt{4x^2 + (\Gamma_1 - \Gamma_2)^2}}},$$

and

$$W(x) = \frac{2x + \sqrt{4x^2 + (\Gamma_1 - \Gamma_2)^2} - \Gamma_1 - \Gamma_2}{2} - x\ln\left[\frac{2x^2 + x\sqrt{4x^2 + (\Gamma_1 - \Gamma_2)^2}}{\Gamma_1\Gamma_2}\right].$$

The saddle-point approximation on the dual problem of current bias allows us to write the voltage distribution in the form $\mathcal{P}(y) = C(y)e^{N_0 W(y)}$, where

$$C(y) = \sqrt{\frac{N_0[4 + (\Gamma_1 - \Gamma_2)^2y^2 + 2\sqrt{4 + (\Gamma_1 - \Gamma_2)^2y^2}]}{2\pi y^2[4 + (\Gamma_1 - \Gamma_2)^2y^2]}},$$

and

$$W(y) = \frac{2 + \sqrt{4 + (\Gamma_1 - \Gamma_2)^2y^2} - (\Gamma_1 + \Gamma_2)y}{2} - \ln\left[\frac{2 + \sqrt{4 + (\Gamma_1 - \Gamma_2)^2y^2}}{\Gamma_1\Gamma_2 y^2}\right].$$

[1] R. Landauer, IBM J. Res. Dev. **1**, 233 (1957); Z. Phys. B: Condens. Matter **68**, 217 (1987).

[2] M. Büttiker, Phys. Rev. B **33**, 3020 (1986); Phys. Rev. Lett. **57**, 1761 (1986).

[3] L. S. Levitov and G. B. Lesovik, Pis'ma Zh. Eksp. Teor. Fiz. **58**, 225 (1993) [JETP Lett. **58**, 230 (1993)]; L. S. Levitov, H. W. Lee, and G. B. Lesovik, J. Math. Phys. **37**, 4845 (1996); For a recent review, see L. S. Levitov, in *Quantum Noise in Mesoscopic Systems*, edited by Yu. V. Nazarov (Kluwer, Dordrecht, 2003).

[4] C. W. J. Beenakker, Rev. Mod. Phys. **69**, 731 (1997).

[5] Yu. V. Nazarov, in *Quantum Dynamics of Submicron Structures*, edited by H. Cerdeira, B. Kramer, and G. Schoen (Kluwer, Dordrecht, 1995), p. 687.

[6] Yu. V. Nazarov, in *Handbook of Theoretical and Computational Nanotechnology*, edited by M. Rieth and W. Schommers (American Scientific, Valencia, CA, 2006).

[7] A. M. S. Macêdo, Phys. Rev. B **66**, 033306 (2002).

[8] A. L. R. Barbosa and A. M. S. Macêdo, Phys. Rev. B **71**, 235307 (2005).

[9] A. M. S. Macêdo and Andre M. C. Souza, Phys. Rev. E **71**, 066218 (2005).

[10] G. C. Duarte-Filho, A. F. Macedo-Junior, and A. M. S. Macêdo, Phys. Rev. B **76**, 075342 (2007).

[11] Yu. V. Nazarov and D. A. Bagrets, Phys. Rev. Lett. **88**, 196801 (2002).

[12] M. Kindermann and Yu. V. Nazarov in *Quantum Noise in Mesoscopic Systems*, edited by Yu. V. Nazarov (Kluwer, Dordrecht, 2003).

[13] M. Kindermann, Y. V. Nazarov, and C. W. J. Beenakker, Phys. Rev. Lett. **90**, 246805 (2003).

[14] P. A. Mello and T. H. Seligman, Nucl. Phys. A **344**, 489 (1980); For a recent review, see P. A. Mello and H. U. Baranger, Waves Random Media **9**, 105 (1999).

[15] P. W. Brouwer and C. W. J. Beenakker, J. Math. Phys. **37**, 4904 (1996).

[16] Yu. Bomze, G. Gershon, D. Shovkun, L. S. Levitov, and M. Reznikov, Phys. Rev. Lett. **95**, 176601 (2005).

[17] S. Gustavsson, R. Leturcq, B. Simovič, R. Schleser, T. Ihn, P. Studerus, K. Ensslin, D. C. Driscoll, and A. C. Gossard, Phys. Rev. Lett. **96**, 076605 (2006).

[18] H. Lee, L. S. Levitov, and A. Yu. Yakovets, Phys. Rev. B **51**, 4079 (1995).

[19] D. A. Bagrets and Yu. V. Nazarov, Phys. Rev. B **67**, 085316 (2003).

[20] A. M. S. Macêdo and A. M. C. Souza, Phys. Rev. B **72**, 165340 (2005).